



Cite this: *Phys. Chem. Chem. Phys.*,
2019, 21, 11488

Correction: Influence of permittivity and energetic disorder on the spatial charge carrier distribution and recombination in organic bulk-heterojunctions

Tim Albes * and Alessio Gagliardi*

DOI: 10.1039/c9cp90135c

rsc.li/pccp

Correction for 'Influence of permittivity and energetic disorder on the spatial charge carrier distribution and recombination in organic bulk-heterojunctions' by Tim Albes *et al.*, *Phys. Chem. Chem. Phys.*, 2017, **19**, 20974–20983.

1 Summary

The authors regret a mistake in their previously published paper and would like to communicate a correction.

Throughout the manuscript, the values for the energetic disorder σ that have been investigated were stated to be 0 meV, 30 meV, 50 meV, and 70 meV. Due to a mistake in the implementation, these values need to be rescaled by a factor of $\sqrt{2}$ and therefore correspond to 0 meV, 42.4 meV, 70.7 meV, and 99.0 meV, respectively. For readability, we will refer to them as 0 meV, 40 meV, 70 meV, and 100 meV in the following.

The results in the original manuscript are correct as presented but the values for the disorder need to be re-labeled throughout the text and in the figures. This correction does not change the overall implications and conclusions, namely the interface charge accumulation and the increased recombination at low permittivity ϵ_r in combination with a large energetic disorder.

2 Detailed correction

In Fig. 1, the charge carrier distribution (CCD) is shown for σ ranging from 40 meV to 100 meV; it replaces Fig. 2 of the original manuscript. The figure is identical except for the labelling of σ . The statement of the figure remains, *i.e.*, large values of σ can make the CCD fluctuate by several orders of magnitude locally.

The quantitative evaluation of interface densities *vs.* bulk densities is shown in Fig. 2 with the corrected axis description for σ ; it replaces Fig. 3 of the original manuscript.

Fig. 4 of the original manuscript remains unchanged, but shows the absolute CCDs for $\sigma = 100$ meV instead of 70 meV.

Fig. 5 of the original manuscript shows the total recombination R_{tot} and corresponding relative amount of geminate recombination $\frac{R_{\text{gem}}}{R_{\text{tot}}}$ for $\sigma = 100$ meV instead of $\sigma = 70$ meV. We have added the results for what should have been Fig. 5 in the

original manuscript, *i.e.* R_{tot} and $\frac{R_{\text{gem}}}{R_{\text{tot}}}$ at 70 meV, in Fig. 3 for an extended parameter set of the recombination rate a_{ehr} ranging between 10^4 s^{-1} and 10^9 s^{-1} . It can be seen from Fig. 3a that, while R_{tot} is considerably smaller than at $\sigma = 100$ meV, it shows the same trend of being strongly dependent on both ϵ_r and a_{ehr} . In particular, also here the change in R_{tot} between slight changes of ϵ_r outweighs orders of magnitude of a_{ehr} and highlights the strong influence of the permittivity on the total recombination. At a disorder of 100 meV, values less than $a_{\text{ehr}} \approx 5 \times 10^4 \text{ s}^{-1}$ were identified at $\epsilon_r = 3.5$ in order to obtain a sufficiently functioning device with $R_{\text{tot}} < 25\%$. At 70 meV, values up to $a_{\text{ehr}} \approx 10^7 \text{ s}^{-1}$ (corresponding to 100 ns of pair recombination time) lead to $R_{\text{tot}} < 25\%$, which represent a more realistic scenario according to what is found by transient absorption spectroscopy (TAS) measurements.¹ Even for recombination times of 1 ns ($a_{\text{ehr}} = 10^9 \text{ s}^{-1}$), the device is still reasonably functioning with 37.47% of all charges recombining. From Fig. 3b it is evident that also at $\sigma = 70$ meV geminate recombination clearly dominates over nongeminate recombination and cannot be neglected as a major loss mechanism.

Department of Electrical and Computer Engineering, Technical University of Munich, Karlstr. 45, 80333 Munich, Germany. E-mail: tim.albes@tum.de



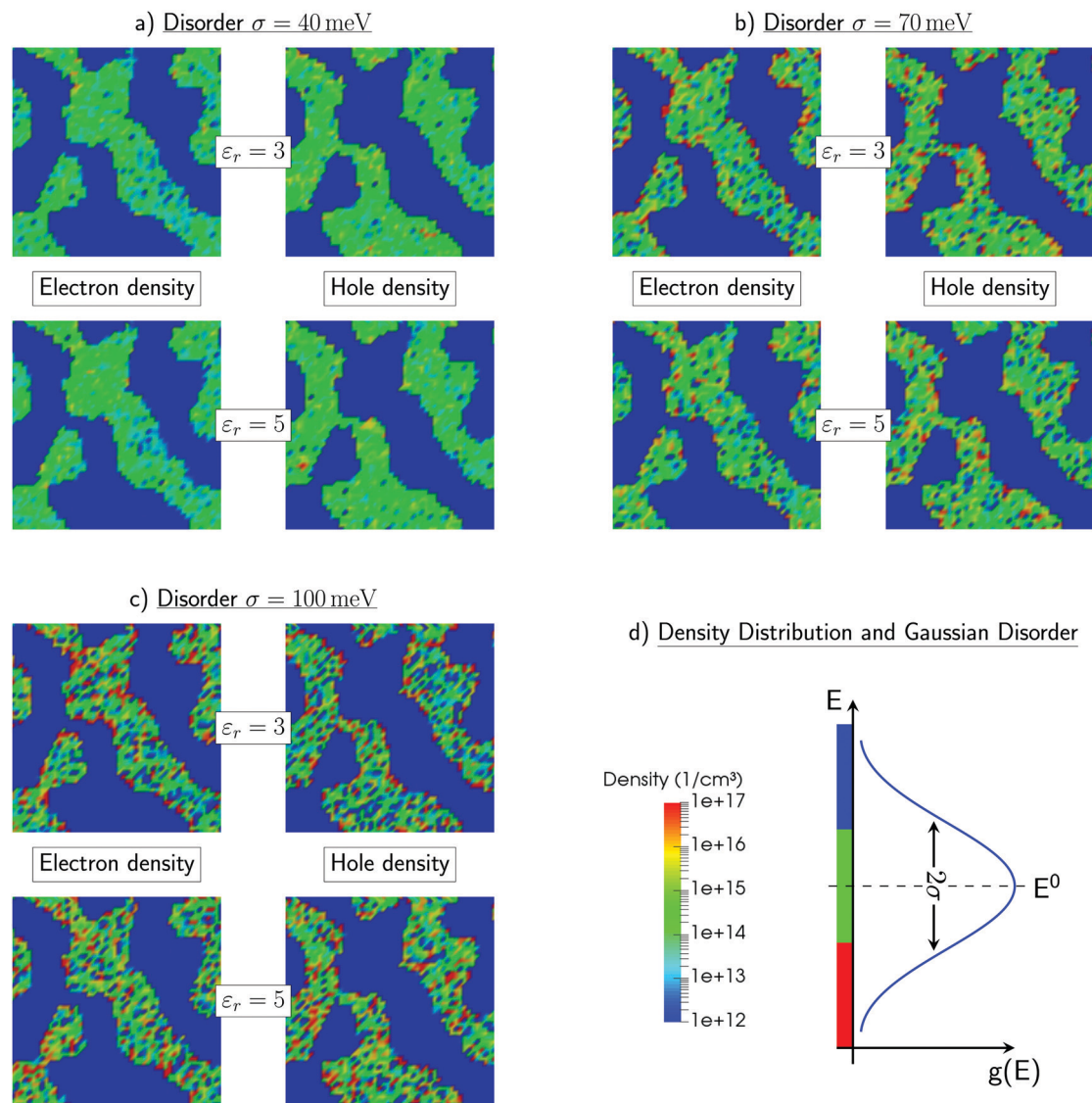


Fig. 1 Electron and hole charge density distributions along a slice through the morphology. All density maps are shown for two cases of low and high permittivity ($\epsilon_r = 3$ and $\epsilon_r = 5$), respectively, and the energetic disorder varies from 40 meV (a) via 70 meV (b) to 100 meV (c). In (d), the corresponding charge density scale and its relationship to the energy levels within the Gaussian density of states is shown.

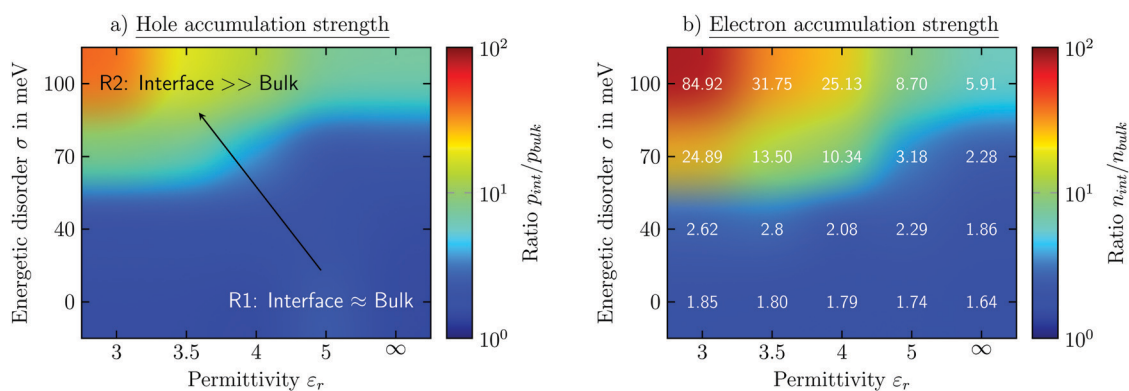


Fig. 2 Ratio of interface to bulk charge densities of holes (a) and electrons (b) for different parameter sets of energetic disorder and permittivity (σ , ϵ_r). High values indicate an inhomogeneous charge distribution with accumulation of charges at the heterojunction interface while a value of 1 represents homogeneous charge distributions of electrons in the acceptor and holes in the donor, respectively. The artificial case of $\epsilon_r = \infty$ (no Coulomb interaction) is added to be able to interpret the effect of disorder alone.

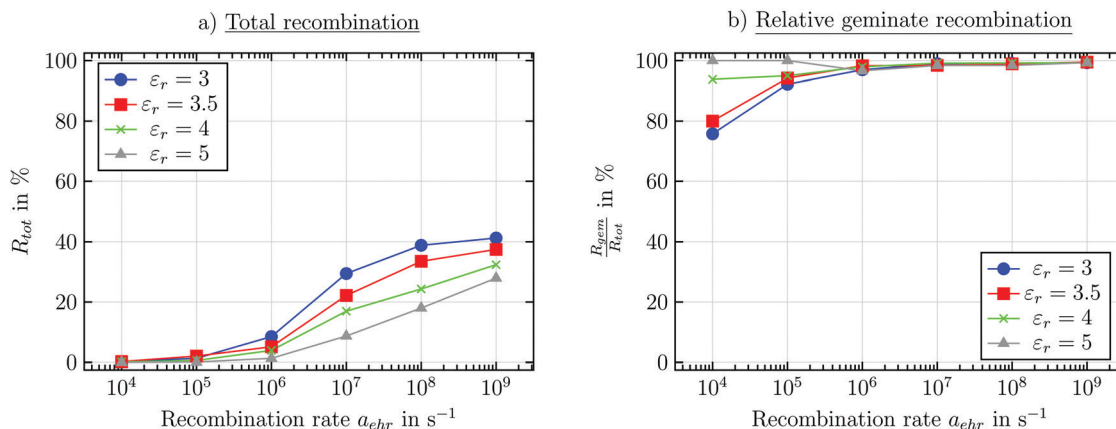


Fig. 3 Amount of total recombination R_{tot} (a) and the corresponding relative part of geminate recombination $R_{\text{gem}}/R_{\text{tot}}$ (b) at $\sigma = 70$ meV depending on a_{ehr} at different values of ϵ_r . A value of $R_{\text{tot}} = 100\%$ means that all charges generated by exciton splitting undergo recombination. A value of $R_{\text{gem}}/R_{\text{tot}} = 100\%$ means that from all recombination events, every single one is geminate and none are nongeminate. All recombination that is not geminate is nongeminate recombination.

Table 1 Effect of permittivity and disorder on short-circuit current density j_{sc} in mA cm^{-2} for $a_{\text{ehr}} = 5 \times 10^4 \text{ s}^{-1}$

σ (meV)	ϵ_r				
	3	3.5	4	5	∞
100	4.62	5.92	6.77	7.62	8.21
70	7.24	7.59	7.33	7.65	8.11
40	7.31	7.44	7.52	7.71	8.24
0	7.53	7.58	7.65	7.75	8.36

Table 2 Effect of permittivity and disorder on short-circuit current density j_{sc} in mA cm^{-2} for $a_{\text{ehr}} = 10^7 \text{ s}^{-1}$

σ (meV)	ϵ_r				
	3	3.5	4	5	∞
100	0.95	2.08	3.24	5.18	8.08
70	5.08	5.72	6.15	6.85	8.10
40	7.45	7.51	7.54	7.69	8.13
0	7.47	7.51	7.66	7.86	8.35

At last, in order to link σ and ϵ_r on the device performance, Table 1 shows the effect of σ and ϵ_r at $a_{\text{ehr}} = 5 \times 10^4 \text{ s}^{-1}$ on the short-circuit current j_{sc} with the corrected values for $\sigma = 0$ meV, 40 meV, 70 meV, 100 meV; it replaces Table 1 of the original manuscript. We have furthermore added the dependence of j_{sc} on σ and ϵ_r for a larger recombination rate of $a_{\text{ehr}} = 10^7 \text{ s}^{-1}$ in Table 2, in order to show the effect at smaller recombination times. The trend is equivalent (*i.e.* the anti-correlation of interface accumulation strength and j_{sc}) but more pronounced, as a larger a_{ehr} induces faster and therefore more recombination.

There are no qualitative changes in the conclusions of the paper. However, considering the corrected results, we can conclude more suitable recombination rates around $a_{\text{ehr}} \approx 10^7 \text{ s}^{-1}$ at an energetic disorder of 70 meV and a permittivity of $\epsilon_r = 3.5$.

Acknowledgements

The authors thank Waldemar Kaiser for spotting the mistake.

The Royal Society of Chemistry apologises for these errors and any consequent inconvenience to authors and readers.

References

- 1 I. A. Howard and F. Laquai, *Macromol. Chem. Phys.*, 2010, **211**, 2063.

